ECCOMAS Congress 2016
VII European Congress on Computational Methods in Applied Sciences and Engineering
M. Papadrakakis, V. Papadopoulos, G. Stefanou, V. Plevris (eds.)
Crete Island, Greece, 5–10 June 2016

ERROR ANALYSIS AND QUANTIFICATION IN NEURON SIMULATIONS

Francesco Casalegno*[1], Francesco Cremonesi[1], Stuart Yates[1], Michael L. Hines[2], Felix Schürmann[1], and Fabien Delalondre[1]

[1]Blue Brain Project
École Polytechnique Fédérale de Lausanne
Campus Biotech, Chemin des Mines 9, 1202 Genève, Switzerland
{francesco.casalegno,francesco.cremonesi,sam.yates,felix.schuermann,fabien.delalondre}@epfl.ch

[2]Yale University
P.O.Box 208001, New Haven, CT 06520-8001, United States
michael.hines@yale.edu

Keywords: Computational Neuroscience, NEURON Software, Error Analysis, Splitting Methods, Stiff Systems, Nonlinear PDEs.

Abstract. *The Blue Brain Project (BBP) uses the NEURON simulator to model the electrical activity of large networks of morphologically detailed neurons. Each individual neuron is typically described by a model that couples the actions of localized membrane mechanisms with an electrical system described by the cable equation on a topology derived from the neuron's dendritic tree. NEURON discretizes the electrical problem in space with finite differences. The system is then solved in time with an implicit Euler or Crank–Nicolson scheme, using Strang splitting to decouple the evolution of the mechanisms from the membrane potential. A typical spatial discretization of a single neuron will have hundreds of elements, and the resulting linear system for the implicit solver is almost tridiagonal.*

In this paper, we present a detailed analysis of the different sources of error arising from the biological and mathematical models underlying NEURON simulations. We provide a detailed account of the mathematical model, identify and evaluate the sources of uncertainty in the biological and numerical models and quantify the errors resulting from the model discretization and from the choice of the integrator. Post-processing based techniques are applied to assess the numerical error in the solution. Of particular interest is the analysis of the discontinuities arising from the pointwise synaptic processes that constitute part of the model, including the effects of voltage-proportional synaptic conductance.

We validate our analysis through a series of numerical experiments on a branched dendrite model incorporating Hodgkin–Huxley distributed ion channels with simple alpha-synapes and biologically realistic AMPA/NMDA activated synapses. This model exhibits the action-potential behaviour with fast dynamics characteristic of a typical simulation of a network of neurons.

1 INTRODUCTION

The assessment of the errors and uncertainties associated with the numerical simulation of mathematical models describing physical phenomena represents a topic of crucial importance in both scientific and engineering research. Several techniques have been developed to provide information on the different sources of error and thereby provide assessments of the accuracy of simulation results.

The motivations for this error analysis are twofold: firstly, confidence in the accuracy and reliability of simulation results requires bounds on the errors of those simulations; secondly, the choice of discretization in space and time should be chosen such that the global error is constrained to lie within certain user-specified bounds. The latter is particularly pertinent when considering the implementation of numerical methods that involve mesh adaptivity and variable step-size integrators.

The results of a numerical simulation are subject to four main classes of error.

- *Modelling errors* are produced when translating the real world physical phenomena into the mathematical model consisting of a set of differential equations.
- *Parameter errors* are due to the uncertainties in the measurements of the quantities necessary for the determination of the parameters of the mathematical model.
- *Discretization errors* arise from the choice of the numerical discretization methods utilized for the numerical solution of the differential equations.
- *Round-off errors* are introduced by the finite-precision arithmetic of the floating point representation used by the computer.

We aim in this paper to address a perceived gap in the literature concerning error bounds and estimates for the results obtained using NEURON simulator[3], the primary tool employed by the BBP for the analysis of the electrical behaviour of morphologically detailed neural networks.

The outline of the paper is as follows. The modelling and parameter errors for this problem are discussed in Section 2. As a prelude to the numerical error analysis, we present in Section 3 a formal statement of the mathematical model. In Section 4 we discuss the space discretization of the differential equations using the finite difference method and we consider the implementation of an error estimator based on the Zienkiewicz–Zhu post-processing technique. In Section 5 we examine the numerical integration methods currently implemented in the NEURON simulator and propose different techniques that allow an improvement in the accuracy of the simulation results. We provide results of numerical experiments in Section 6, using a simplified dendrite model with a single branching point. While consideration of round-off error is important, we do not address it in this paper.

2 MODELLING AND PARAMETER ERRORS

Three simplifying assumptions underlie the derivation of the mathematical model of neuronal electrical behaviour used by NEURON: the Maxwell quasi-static approximation, the 1-D approximation, and the distribution of ion channels and point processes.

The quasi-electrostatic approximation to Maxwell's equations assumes that inductive effects and wave propagation delays are negligible (see for example [13]). In the NEURON model, it is assumed the only significant capacitive phenomena are those caused by the difference in extra- and intra-cellular potentials at the membrane of the dendrite, and that the frequencies involved are sufficiently low that the behaviour lies in the quasi-electrostatic domain. This simplification was first justified by the research on electro-physiological systems of Plonsey and Heppner [16]. However, Bossetti et al. [2] have recently argued that in the case of short and fast impulses the

argument of [16] may be undermined. To test their ideas, Bossetti et al. relaxed the quasi-static assumption and simulated the resulting inhomogeneous Helmholtz equation. Their results show that whilst propagation and induction effects can be quite safely neglected, the system exhibits a higher sensitivity with respect to capacitive and conductive effects. In any case, numerical results obtained by the authors find a relative error of 5 to 13% for pulse widths within the range of typical neural events (25µs to 1 ms).

The unbranched sections of the dendritic tree of a neuron are typically much thinner than they are long, and so are amenable to a one-dimensional approximation that represents the potential within the dendrite as a function of the axial distance along a section. This assumption leads to a description in terms of electrical cable theory. A study of Lindsay et al. [12] has criticized this approach by observing that dendritic currents have an essential radial component that may not be neglected in the case of dendritic tapering. Lindsay et al. compared numerical simulations of the simplified 1-D model with ones incorporating higher order perturbations capturing the radial variation, and found that when synaptic input is weighted towards the distal end of the dendrite, the generated spike trains showed statistically significant differences between the models. On the other hand, if the weighting is towards the proximal end of the dendrite the spike trains are statistically indistinguishable, even though the actual firing patterns might differ.

Lastly, the third approximation concerns the distribution of ion channels and synapses. Ion channels are proteins that reside on the membrane of the cell, and are responsible for gating the flow of charged ions through the cell membrane. As such, ion channels are discrete phenomena, giving a spatially localised contribution to the transmembrane current by allowing single particles of charged ions to pass through their selectivity filters. As a consequence of the conductance based formalism these ion channels are not modelled individually. Rather, NEURON operates under the assumption that the contributions of these channels can be averaged across a section of dendrite where the density of their distribution can be considered uniform. Synapses, on the other hand, are modelled as discrete processes but are located on the dendrite only at nodes arising from the spatial discretization.

Once the appropriate model has been chosen for representing a neuron, the computational neuroscientist is still required to specify the value of some input parameters. Here we consider two sources of parameter error: morphology reconstruction and matching electrophysiological data.

Computer reconstructions are commonly used to provide cell-type specific morphologies as input to neural simulations. In this process, an expert controls a microscope to analyse a set of brain slices that have been stained in order to enhance visibility of cellular structures such as the soma, dendrites and axons. Unfortunately, during staining an error due to tissue shrinkage can be introduced; [18], for example, observed a shrinkage of approximately 10% in the X and Y directions and 25% in slice thickness. The work of Blackman et al. [1] investigated the effects of shrinkage and other reconstruction artefacts on the results of computer simulations conducted using the NEURON software. They consider two popular reconstruction techniques: biocytin histology and two-photon imaging. The authors identify some systematic defects introduced by both techniques. They note, however, that clustering of morphological types was successful with both techniques, and that electrophysiological parameters that could be affected by morphological properties of the dendrite, such as length constants, did not seem to be affected significantly by the uncertainty introduced by the two methods. Although recent techniques allow 3-D imaging of intact brains [4], many computer reconstruction techniques in use today require the reduction of the three dimensional brain to a set of two-dimensional slices. This process carries an intrinsic source of error: not only may some branches may be

severed, distorted or deformed during the slicing process; the human expert or image reconstruction software may also make mistakes while connecting multiple two dimensional slices into a three dimensional shape. It is important to consider these sources of error even if they are extremely difficult to quantify, as a neuron's morphology plays an important role in determining its electrophysiological properties [11].

Just as the different components of a computer chip give rise to meaningful emergent behaviour by exploiting differences in their electrical behaviours, it is thought that the ability of a neuron to *integrate* in a very specific way the synaptic input from other cells is at the core of the brain's ability to perform computations. As such, the main goal of developing a detailed neuron model is to be able to reproduce with high fidelity its experimentally measured electrophysiological behaviour, thus distinguishing it from other cells. Often this requires a two step process, which begins by obtaining valid experimental data. In this phase, errors may come from measurement sensitivity and noise. The comprehensive guide on patch clamp experiment setups [19] estimates that a realistic value for noise in patch clamp experiments is around 0.2 pA rms, which considering a typical cell resistance of 100 MΩ leads to a negligible noise amplitude of around 20 µV. Moreover, a typical value of the resolution of such experimental setups is in the order of 0.01 pA to 1 pA, which leads again to a resolution on the membrane potential of roughly 1 µV to 100 µV.

Once the experimental data has been obtained, computational neuroscientists often use an optimization algorithm to find the best set of model parameters to fit such data. Recently the community has shown interest in the use of evolutionary algorithms (see e.g. [5]). As fitting the raw experimental observations can be difficult or overwhelmingly costly in some cases, more and more focus is being placed on feature-based fitting, which consists of trying to replicate a set of secondary measures that can be computed from the experimental data (e.g. a neuron's firing rate under a certain stimulation protocol) rather than replicating the raw data directly (see [20] for a review). These optimization algorithms can suffer from intrinsic uncertainties and errors: they may get stuck in local minima, produce results that are not biologically plausible, incorrectly overfit the data or fail to replicate certain aspects of a neuron's electrophysiology due to a poor choice of the features. In addition, it is hard to quantify the degree of uncertainty in the raw experimental data that will affect the final uncertainty of the input parameters.

3 MATHEMATICAL MODEL

Before discussing numerical recipes for the simulation of neural circuits and error estimation, we need to clearly state the mathematical expression of the biological model. In this section we present the complete formulation of the equations typically solved by NEURON.

The behaviour of electrical signals in neurites is described by *cable theory*, which is derived from an electrical model with a constant axial resistivity and a leaky capacitive membrane. While a great variety of ion channel models are supported by NEURON, we restrict ourselves to the Hodgkin–Huxley model of voltage-gated sodium and potassium ion channels [10].

The model is defined over a domain Ω, comprising a disjoint collection of closed intervals of the real line; each interval corresponds to an unbranched section of dendrite, and the branching structure will be captured by additional boundary conditions applied at the interval end-points. Within the cable theory model, the membrane potential $v(x,t)$ is described by a variable depending only on time t and position x on the axis. In addition to these variables, we have to consider some quantities regulating the behaviour of the ion channels. The ion channel states in the Hodgin–Huxley model are described by dimensionless quantities $n(x,t)$, $m(x,t)$, and $h(x,t)$ with a voltage-dependent evolution in time. Finally, we consider the contribution of

discrete synaptic receptors on the surface of a section, which are governed by a dimensionless per-synapse state $y(t)$.

3.1 Differential equations

The governing equations for the systems are obtained through a balancing of trans-membrane currents and axial currents. The resulting system is the *cable equation* with additional terms capturing the ion channel currents,

$$\begin{aligned} 10^{-3} c_m \frac{\partial v}{\partial t} = & \frac{10^4}{2aR} \frac{\partial}{\partial x} \left(a^2 \frac{\partial}{\partial x} v \right) \\ & - g_{\mathrm{K}} n^4 (v - e_{\mathrm{K}}) - g_{\mathrm{Na}} m^3 h (v - e_{\mathrm{Na}}) - g_l (v - e_l) \\ & - \frac{10^2 g_{syn}(y, v)}{2\pi a} \delta_{syn}(x)(v - e_{syn}), \end{aligned} \tag{1}$$

where: the membrane potential v is expressed in mV; a is the dendrite radius [µm]; c_m is the membrane specific capacitance [µF·cm^{-2}]; R is the cytoplasmic resistivity [Ω·cm]; g_{K}, g_{Na}, g_l, and $g_{syn}(y, v)$ are specific conductances [S·cm^{-2}] (the latter depending on other variables); e_{K}, e_{Na}, e_l, and e_{syn} are reversal potentials [mV]; and $\delta_{syn}(x)$ is a Dirac delta centred on the synaptic receptor location x_{syn}.

The evolution of the ion channels states is described by nonlinear functions $\alpha_\times(v)$ and $\beta_\times(v)$ derived by Hodgin and Huxley [10],

$$\begin{aligned} \frac{\mathrm{d}n}{\mathrm{d}t} &= \alpha_n(v)(1 - n) - \beta_n(v) n, \\ \frac{\mathrm{d}m}{\mathrm{d}t} &= \alpha_m(v)(1 - m) - \beta_m(v) m, \\ \frac{\mathrm{d}h}{\mathrm{d}t} &= \alpha_h(v)(1 - h) - \beta_h(v) h. \end{aligned} \tag{2}$$

The evolution of the synaptic receptor state can be described by an ordinary differential equation (ODE) of the form

$$\frac{\mathrm{d}y}{\mathrm{d}t} = \gamma(y) \tag{3}$$

where both the function $\gamma(y)$ and the behaviour of the specific conductance g_{syn} depend on the kind of synapse to be modelled. We consider here two different kinds of synaptic receptors:

- *Alpha-synapses* (see [3]) are simplified models, where the conductance $g_{syn}(y)$ is only dependent on the synapse state y.
- *Deterministic AMPA/NMDA-synapses* (described in [14]) are more realistic models, in which the conductance $g_{syn}(y, v)$ depends as well on the membrane potential to account for magnesium blocking of the NMDA receptor.

3.2 Initial and boundary conditions

The system of differential equations formed by (1), (2), and (3) are to be combined with initial and boundary conditions. For given initial conditions on the membrane potential

$$v|_{t=t^0} = v^0 \tag{4}$$

we recover the initial values for the ion channels states by considering the steady state solution of Equation (2),

$$n|_{t=t^0} = \frac{\alpha_n(v^0)}{\alpha_n(v^0)+\beta_n(v^0)}, \quad m|_{t=t^0} = \frac{\alpha_m(v^0)}{\alpha_m(v^0)+\beta_m(v^0)}, \quad h|_{t=t^0} = \frac{\alpha_h(v^0)}{\alpha_h(v^0)+\beta_h(v^0)}. \tag{5}$$

As for the boundary conditions for the membrane potential, we impose the balance of the axial current to obtain natural boundary conditions on the boundary points of each unbranched section Ω_i of the dendrite. We have to distinguish different cases depending on the position of the boundary point x_b within the dendritic tree, that is whether the boundary of the section is a terminal end of the dendrite or if it communicates with other sections through a branching (see [9]).

- On a *terminal point* x_b of the dendrite we have homogeneous conditions

$$\left.\frac{\partial v}{\partial x}\right|_{x=x_b} = 0. \tag{6}$$

- On a *branching point* x_b (see Figure 1a) the boundary conditions link together the gradients of the membrane potentials on the section Ω_A preceding the branching and on the sections Ω_{B_1} and Ω_{B_2} following it,

$$\left(a^2\frac{\partial v}{\partial x}\right)\Big|_{x=x_b}^{A} = \left(a^2\frac{\partial v}{\partial x}\right)\Big|_{x=x_b}^{B_1} + \left(a^2\frac{\partial v}{\partial x}\right)\Big|_{x=x_b}^{B_2}. \tag{7}$$

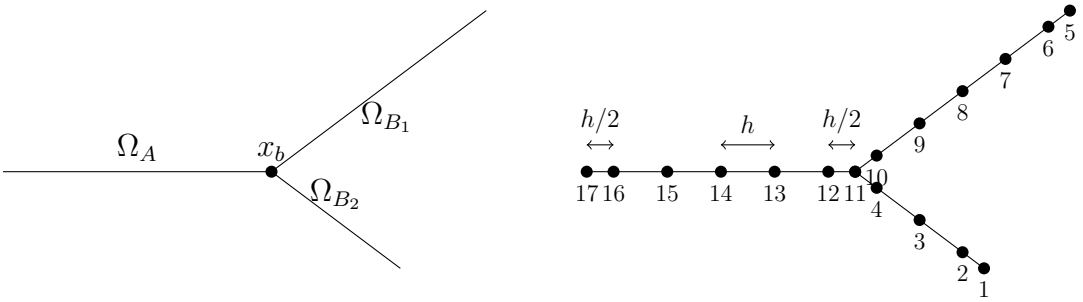

(a) Branched dendrite

(b) Space discretization and node ordering

Figure 1: Branched dendrite and its space discretization with an example of the node ordering used in NEURON to avoid fill-in during Gaussian elimination.

4 DISCRETIZATION IN SPACE

The strategy implemented in NEURON to solve (1) numerically is known as the *method of lines* (see [7]), which transforms the partial differential equation (PDE) into a system of ODEs through a suitable space discretization and then integrates the latter in time using some numerical scheme. In this section we discuss the discretization in space, while the integration in time is analysed in Section 5.

4.1 Numerical methods

The differential equations (1) constituting the mathematical model are discretized by finite differences to form a system of ODEs. On a given unbranched section, the nodes x_j of the mesh are chosen with an equal spacing h except for the boundary nodes where the spacing is $h/2$, as shown in Figure 1b.

It is important to mention that the numbering of the nodes of the dendrite has a critical role in the structure of the linear system to be solved after space discretization. NEURON adopts the node ordering scheme described in [9], such that branches that are further away from the soma have lower node indexes (see Figure 1b). This gives rise to a global stiffness matrix for the dendrite which is almost tridiagonal and which can be efficiently solved using an ad hoc version of Thomas algorithm with linear complexity, as the Gaussian elimination step requires the same number of arithmetic operation for a tree of N nodes as for a cable with N nodes.

Particular care must be paid to the second order term and to the Dirac delta when applying the finite differences discretization. Among the different finite difference approximations that are possible for the second order term, NEURON uses the discretization

$$\frac{\partial}{\partial x}\left(a^2(x)\frac{\partial v}{\partial x}(x)\right)\bigg|_{x=x_j} \approx \frac{1}{h}\left(a^2_{j+1/2}\frac{v_{j+1}-v_j}{h} + a^2_{j-1/2}\frac{v_{j+1}-v_j}{h}\right). \tag{8}$$

As for the Dirac delta term, NEURON uses the discretization

$$\delta_{syn}(x)v(x)\big|_{x=x_j} \approx \frac{\delta_{j,j_{syn}}}{h}v_j, \tag{9}$$

where $\delta_{j,j_{syn}}$ is the Kronecker delta and j_{syn} is the index of the node of the synaptic receptor.

Note that the finite difference scheme as described above coincides, up to higher order terms, with a finite element scheme with piecewise linear elements (see [17]). As a consequence, the order of convergence in the $L^2(\Omega)$ norm for the numerical solution v_h and its gradient ∇v_h can be expected to be quadratic and linear respectively. In addition, the equivalence of this finite difference scheme to the finite element method allows us to use error estimation techniques suited to finite element algorithms.

4.2 Error estimation

By interpreting the finite difference discretization used in NEURON as a variant of the finite element method, we can consider applying classical error estimation techniques for finite element methods. Residual-based estimators cannot be used, however, as the PDE (1) contains a non-integrable Dirac function. Instead, we use a Zienkiewicz–Zhu (ZZ) post-processing estimator based on a superconvergent patch recovery, as described in [21]. This method has been proved to be amongst the most robust error estimators available.

In our case, the superconvergent patch recovery technique is used to compute, from the numerical solution v_h of the finite difference scheme, a *better gradient* Gv_h converging quadratically to the exact gradient ∇v in the $L^2(\Omega)$ norm. The exact error in the gradient is thus approximated using

$$\|Gv_h - \nabla v_h\|_{L^2(\Omega)} = \|\nabla v - \nabla v_h\|_{L^2(\Omega)} + O(h^2). \tag{10}$$

The better gradient is a piecewise linear function computed locally using the values of the discrete solution v_h on triples of consecutive nodes x_{j-1}, x_j, and x_{j+1}. It is then clear that

this procedure provides worse estimates on boundary elements. Furthermore, we remark that this patch recovery fails where the exact solution contains a singularity (see Figure 2a). In order to adapt the method to our case, we split each section containing a synaptic receptor into subsections where the solution is smooth and then apply ZZ post-processing on each subsection.

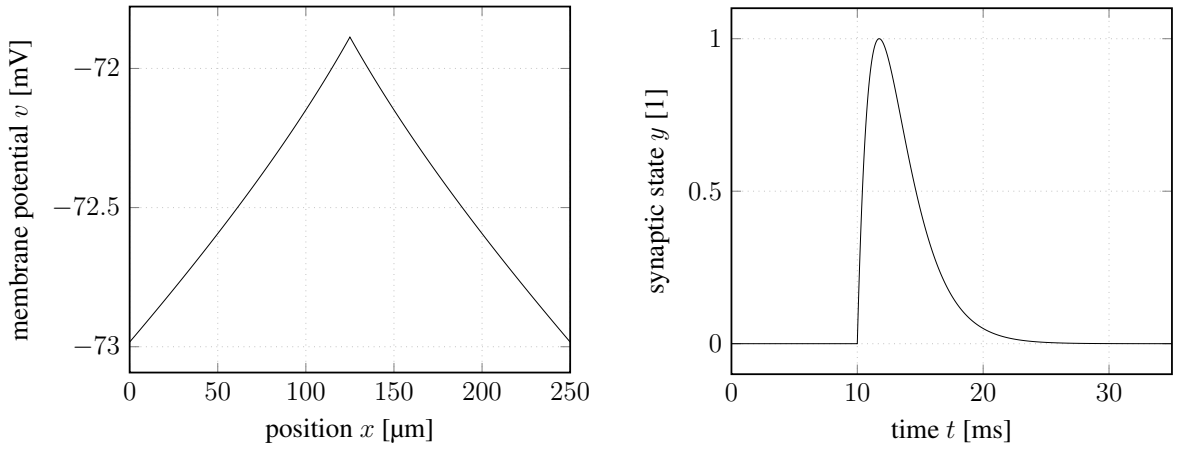

(a) Singularity in space.

(b) Singularity in time

Figure 2: Singularities in the system: (a) membrane potential on a unbranched section of the dendrite with a singularity on the synaptic receptor ($x_{syn} = 125$ µm); (b) synaptic state over time with a singularity at spike arrival ($t_{rec} = 10$ ms).

5 INTEGRATION IN TIME

After the space discretization performed with the finite difference method described in Section 4, we obtain from (1) a system of ODEs that can be written together with (2) and (3) in the form

$$\begin{cases} \dfrac{\mathrm{d}\boldsymbol{v}}{\mathrm{d}t} = A(\boldsymbol{n}, \boldsymbol{v}, y)\boldsymbol{v} + a(\boldsymbol{n}, \boldsymbol{v}, y), \\ \dfrac{\mathrm{d}\boldsymbol{n}}{\mathrm{d}t} = B(\boldsymbol{v})\boldsymbol{n} + b(\boldsymbol{v}), \\ \dfrac{\mathrm{d}y}{\mathrm{d}t} = \gamma(y). \end{cases} \tag{11}$$

where $\boldsymbol{v}$ is the vector of the approximated membrane potential values v_j, and $\boldsymbol{n}$ is the vector of the gate states values n_j, m_j, and h_j at the mesh nodes x_j. We now discuss how to integrate (11) numerically and estimate the error in time. More specifically, we firstly present the numerical methods currently implemented in NEURON and we then suggest some techniques to improve their order of convergence and speed.

5.1 Numerical methods: current NEURON implementation

The structure of the system of ODEs (11) is particularly important for the choice of the numerical integration method. As mentioned in Section 4, the matrix $A(\boldsymbol{n}, \boldsymbol{v}, y)$ has a particularly convenient almost tridiagonal form, while it is easy to see that $B(\boldsymbol{v})$ is purely diagonal.

Another important consideration for the choice of the method is the stiffness of the system. The matrix $A(\boldsymbol{n}, \boldsymbol{v}, y)$ is obtained from the space discretization of the parabolic PDE (1) using the method of lines and thus it has a very large negative eigenvalue whose magnitude scales as

$1/h^2$ (see [7]), so that the ODE for $\boldsymbol{v}$ is highly stiff. For the particular form of the Hodgin–Huxley model's functions $\alpha_\times(v)$ and $\beta_\times(v)$ in (2) it can be shown that the matrix $B(\boldsymbol{v})$ has a spectral radius smaller than 10, so that the ODE for $\boldsymbol{n}$ non-stiff.

The system of ODEs (11) is highly nonlinear but is amenable to being split into two subsystems for $\boldsymbol{v}$ and for $\boldsymbol{n}$ and y respectively, to simplify its numerical integration. The idea of splitting methods (see [7]) is to approximate the exact flow φ_τ of an ODE $\mathrm{d}z/\mathrm{d}t = f^A(z) + f^B(z)$ using a composition of the flows of the partial ODEs as

$$\varphi_\tau \approx \varphi^A_{a_1\tau} \circ \varphi^B_{b_1\tau} \circ \cdots \circ \varphi^A_{a_J\tau} \circ \varphi^B_{b_J\tau}. \tag{12}$$

Goldman and Kaper [6] proved that for every splitting method of the form of (12) with order $p > 2$ there exist two indices $1 \leq j_1, j_2 \leq J$ such that $a_{j_1}, b_{j_2} < 0$ and thus the resulting method in unstable for stiff systems. Due to this order barrier, the second order *Strang splitting*

$$\varphi_\tau = \varphi^A_{\tau/2} \circ \varphi^B_\tau \circ \varphi^A_{\tau/2} + O(\tau^3) \tag{13}$$

is optimal. This is the splitting adopted in NEURON for the integration in time of the system of ODEs.

Let us now firstly assume that the synaptic receptor is modelled with a conductance $g_{syn}(y)$ independent from the membrane potential. Then we can drop the dependence on $\boldsymbol{v}$ of the terms on the right-hand side of the ODE for $\boldsymbol{v}$ and at each time step we have to compute $\boldsymbol{v}^{k+1} \approx \boldsymbol{v}(t^{k+1})$ and $\boldsymbol{n}^{k+1/2} \approx \boldsymbol{n}(t^{k+1/2})$, $y^{k+1/2} \approx y(t^{k+1/2})$ by solving

$$\begin{aligned}
\frac{\mathrm{d}\boldsymbol{n}}{\mathrm{d}t} &= B(\boldsymbol{v}^k)\boldsymbol{n} + b(\boldsymbol{v}^k), && t \in [t^{k-1/2}, t^{k+1/2}], \\
\frac{\mathrm{d}y}{\mathrm{d}t} &= \gamma(y), && t \in [t^{k-1/2}, t^{k+1/2}], \\
\frac{\mathrm{d}\boldsymbol{v}}{\mathrm{d}t} &= A(\boldsymbol{n}^{k+1/2}, y^{k+1/2})\boldsymbol{v} + a(\boldsymbol{n}^{k+1/2}, y^{k+1/2}), && t \in [t^k, t^{k+1}].
\end{aligned} \tag{14}$$

The value of y^{k+1} can be often computed exactly, since $y(t)$ is typically a damped exponential or a similar function. The values of $\boldsymbol{v}^{k+1}$ and $\boldsymbol{n}^{k+1/2}$ could be computed by solving exactly (14), since after the splitting their ODEs are fully linearized. However the exact solution requires the computation of the exponential of A and B—the matrix A has a tridiagonal pattern, so its exponential is dense and its computation would be particularly expansive; on the other hand, the matrix B is diagonal so it is possible to compute its exponential with little effort. In NEURON, therefore, $\exp(\tau B)$ is computed exactly, whilst a Padé approximation (see [8]) is used to avoid the computation of $\exp(\tau A)$. Strang splitting introduces a second order error in time, therefore only Padé approximations of order $p \leq 2$ are convenient. Moreover, a stable approximation has to be chosen due to the stiffness of the ODE. In NEURON the exponential is approximated using the second order approximation equivalent to the Crank–Nicolson method

$$R_{CN}(\tau A) = \left(I - \tfrac{\tau}{2}A\right)^{-1}\left(I + \tfrac{\tau}{2}A\right) = \exp(\tau A) + O(\tau^3). \tag{15}$$

This second order approximation is obtained in NEURON by computing a half step of the first order Padé approximation $R_{BE}(\tau A) = (I - \tau A)^{-1}$ corresponding to backward Euler, and then recovers the Crank–Nicolson approximation through the relationship

$$R_{CN}(\tau A) = 2R_{BE}(\tfrac{\tau}{2}A) - I. \tag{16}$$

The resolution of an almost tridiagonal system (which can be solved using a modified Thomas algorithm with linear complexity) is thereby performed only once while maintaining a second order method.

Let us now consider the case of the more realistic AMPA/NMDA synapse model, where the conductance $g_{syn}(y, \boldsymbol{v})$ depends as well on the membrane potential. In this case the ODE for $\boldsymbol{v}$ contains a nonlinear term

$$\frac{\mathrm{d}\boldsymbol{v}}{\mathrm{d}t} = A(\boldsymbol{n}^{k+1/2}, y^{k+1/2}, \boldsymbol{v})\boldsymbol{v} + a(\boldsymbol{n}^{k+1/2}, y^{k+1/2}, \boldsymbol{v}), \quad t \in [t^k, t^{k+1}]. \tag{17}$$

The current implementation in NEURON uses the value $\boldsymbol{v}^k$ (which is known) to simplify (17) and avoid nonlinearities, obtaining

$$\frac{\mathrm{d}\boldsymbol{v}}{\mathrm{d}t} = A(\boldsymbol{n}^{k+1/2}, y^{k+1/2}, \boldsymbol{v}^k)\boldsymbol{v} + a(\boldsymbol{n}^{k+1/2}, y^{k+1/2}, \boldsymbol{v}^k), \quad t \in [t^k, t^{k+1}]. \tag{18}$$

In Section 6 we see that this technique unfortunately has the drawback of reducing the order of convergence of the numerical integration scheme from quadratic to linear.

5.2 Numerical methods: suggested improvements

We now want to present some numerical integration techniques to improve the results obtained using the aforementioned current implementation of NEURON. Our suggestions are aimed at enhancing both the speed of the integration in time and the accuracy of the results.

We mentioned above that NEURON, in its current implementation, integrates the ODE for $\boldsymbol{n}$ in (14), by computing the matrix exponential $\exp(\tau B)$ exactly. Such a high precision computation is however unnecessary, since the global accuracy of the method cannot exceed second order in time. As a consequence we can consider using a cheaper Padé approximation for the exponential of B. In this case the ODE is non-stiff, so we can choose an explicit approximation. The explicit second order Padé approximation of the exponential corresponds to the Heun method

$$R_H(\tau A) = I + \tau A + \tfrac{\tau}{2}A^2 = \exp(\tau A) + O(\tau^3). \tag{19}$$

This strategy does not reduce the order of convergence of the numerical method and at the same time avoids the computation of exponential functions performed in NEURON, resulting in a more efficient integration scheme.

Regarding the integration of realistic model of synapses with a conductance $g_{syn}(y, \boldsymbol{v})$ dependent on the potential, such as for the AMPA/NMDA model, we observed that the current implementation of NEURON simplifies the system of ODEs by eliminating the nonlinear terms with a technique that destroys the second-order accuracy of the numerical integration (see Section 6). We suggest here a different approach that allows us to preserve the quadratic order of convergence even in case of voltage dependent synaptic conductances. The idea is to use one Newton–Raphson iteration to solve the nonlinear equations corresponding to backward Euler with step size $\tau/2$; a second order method corresponding to Crank–Nicolson) is hence obtained by applying the formula (16) to the result. We point out that this strategy still requires only the solution of an almost tridiagonal system, so that no additional computational cost is required, while the accuracy of the method is significantly improved, as we show in Section 6.

Finally, a critical point is represented by the discontinuity in the ODE $\mathrm{d}y/\mathrm{d}t = \gamma(y)$. Indeed, $\gamma(y) = 0$ in the intervals between inter-spike intervals; when a spike is received at time $t = t_{rec}$ from a presynaptic neuron, $\gamma(y)$ presents then a discontinuity, generating a singularity in y (see

Figure 2b) and hence in the other variables of the system. It has been largely observed (see [7]) that crossing a discontinuity without some specific handling can introduce significant errors. In our simulations we observed (as we show in Section 6) that the current implementation of NEURON produces a global error which is $O(\tau)$ instead of $O(\tau^2)$ in every simulation that includes spike arrivals, as a result of this lack of adequate discontinuity handling. As shown by Hairer [7], the best way to compute a solution crossing a discontinuity consists in implementing an integrator that stops the computation at the point of discontinuity and restarts it with the new value of the right-hand side of the ODE. This technique is considerably more accurate than even a variable step size integrator with automatic error control. We therefore adopted this method for the handling of discontinuity, and the numerical results discussed in Section 6 demonstrate the recovery of a global $O(\tau^2)$ convergence.

5.3 Error estimation

Both local error (i.e. after one time step) and global error (i.e. at the end of the simulation time T) can be estimated using Richardson extrapolation. Given a step size τ, the global error in the numerical solution $\boldsymbol{v}_\tau(T)$ can be estimated from the numerical solution $\boldsymbol{v}_{\lambda\tau}(T)$ computed with a step size λ times larger (in our simulations we use $\lambda = 2$). These calculations, being independent, can be computed efficiently in parallel. A superconvergent approximation is then obtained using Richardson extrapolation

$$\boldsymbol{v}_{R(\tau)}(T) = \frac{\lambda^2 \boldsymbol{v}_\tau(T) - \boldsymbol{v}_{\lambda\tau}(T)}{m^2 - 1}, \tag{20}$$

and the exact global error is then approximated by

$$\|\boldsymbol{v}_{R(\tau)}(T) - \boldsymbol{v}_\tau(T)\|_2 = \|\boldsymbol{v}(T) - \boldsymbol{v}_\tau(T)\|_2 + O(\tau^3). \tag{21}$$

6 NUMERICAL RESULTS

To test the validity of the different numerical methods discussed in Section 4 and 5 we considered a simple model of a branched dendrite with uniform space discretization, such as the one shown in Figure 1b. The codes have been implemented in GNU Octave to replicate the results obtained in the current implementation of NEURON and to test the new ideas proposed here.

We first checked the order of convergence in space of the method, given the particular boundary condition at branching nodes (connecting the values of v on different sections) and the synapse point processes that produce singularities in the solution. The numerical results (see Figure 3) confirm that with respect to the L^2 norm, quadratic convergence in v_h and linear convergence in ∇v_h is preserved.

Regarding the order of convergence in time, we tested the different techniques presented in Section 5 first with alpha-synapses (where $g_{syn} = g_{syn}(y)$) and then with AMPA/NMDA synapses (where $g_{syn} = g_{syn}(y, v)$), and measured empirically the order of convergence of the global error in $\boldsymbol{v}_\tau(T)$.

In Figure 4a we show the results obtained for alpha-synapses. In particular, we see that without discontinuity handling, such as in the current NEURON implementation, the order of convergence is severely degraded. Our technique of discontinuity detection with stopping and restarting of the integration at the spike arrival time t_{rec} allows us to recover a full order 2 convergence.

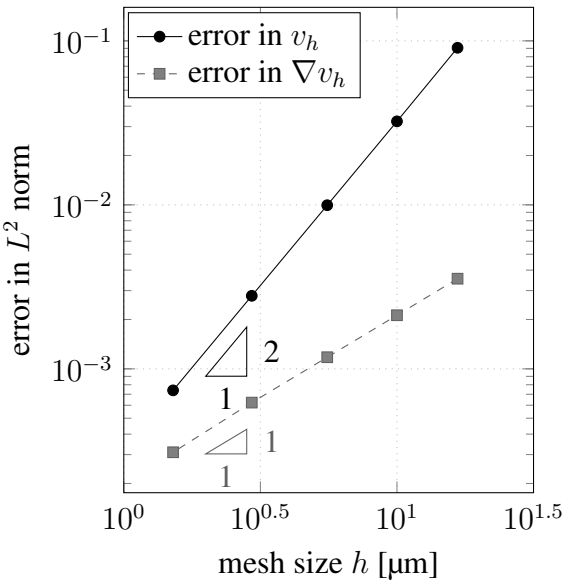

Figure 3: Convergence in space looking at the errors $\|v - v_h\|_{L^2}$ and $\|\nabla v - \nabla v_h\|_{L^2}$.

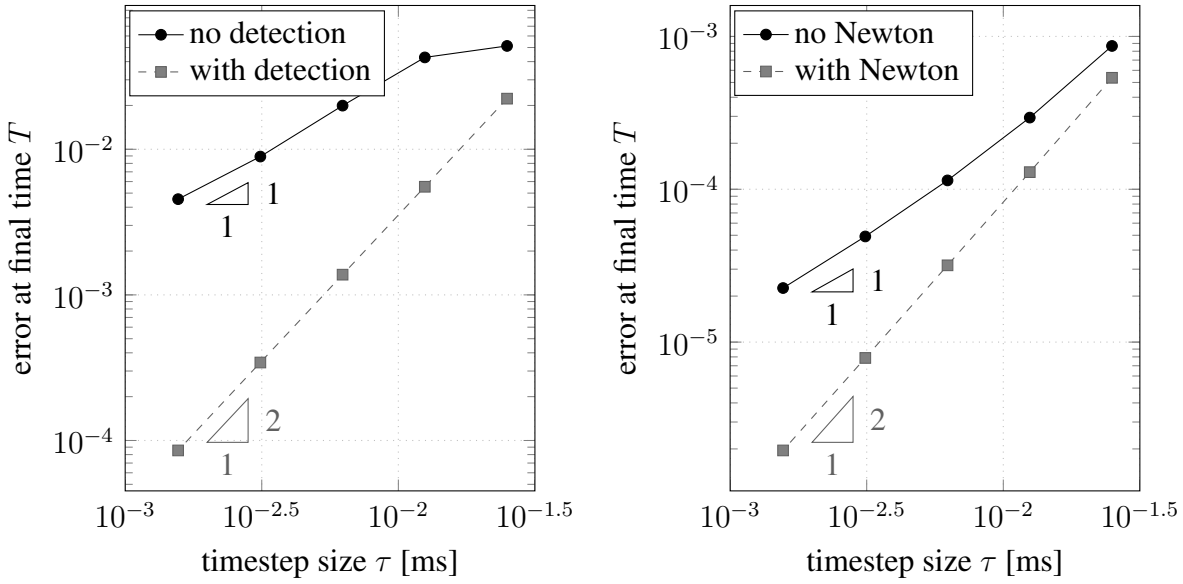

(a) Alpha-synapse

(b) AMPA/NMDA synapse

Figure 4: Convergence in time looking at the global error $\|\boldsymbol{v}(T) - \boldsymbol{v}_\tau(T)\|_2$ for different kinds of synapses and different numerical methods.

Figure 4b presents the results for the more realistic AMPA/NMDA synapse model. In this case we only considered methods incorporating the discontinuity detection technique. The simple technique adopted in NEURON (see Section 5.1) to resolve the nonlinearity still present after Strang splitting is shown to fail, reducing the method's convergence to order 1. However, the method we proposed based on performing only one step of Newton iteration to solve the nonlinear equation proves to be effective and restores quadratic convergence.

To summarise, the quadratic convergence in time is maintained through the use of the integration methods described in Section 5.2 that more effectively handle discontinuities and

nonlinearities in the system of ODEs, and is preserved when the computationally expensive exponential of τB is replaced by the much cheaper Heun method (19).

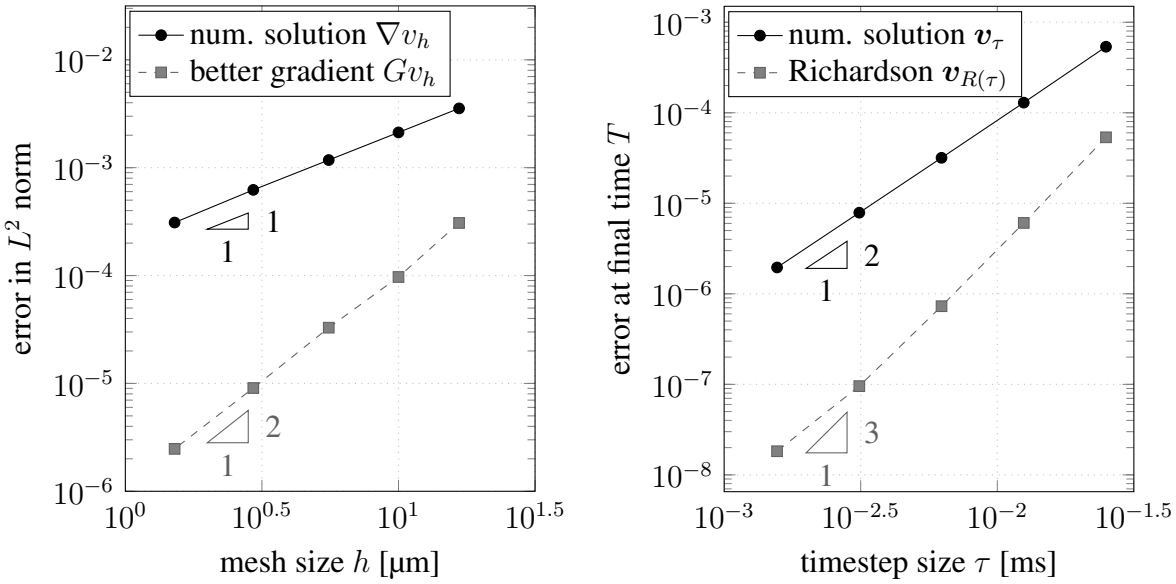

(a) ZZ patch recovery

(b) Richardson extrapolation

Figure 5: Superconvergence for error estimator in space (Zienkiewicz–Zhu patch recovered gradient) and in time (Richardson extrapolation).

Finally, we tested the validity of the post-processing methods for the estimation of the errors in space and time. In general, we define the *efficiency index* of an error estimator err^* for the true error err as the ratio

$$\theta = \frac{err^*}{err}. \tag{22}$$

It is desirable that the efficiency index $\theta \to 1$ at least linearly as the discretization is more and more refined. A sufficient condition to attain this goal is that the post-processed *better* solution is superconvergent with respect to the bare numerical solution itself. In Figure 5 we can can see that the better gradient obtained using Zienkiewicz–Zhu patch recovery and the better trajectory obtained using Richardson extrapolation are superconvergent with order $O(h^2)$ and $O(\tau^3)$, respectively, while the bare numerical solution converge with order $O(h)$ and $O(\tau^2)$, respectively. This validates our choice of error estimator.

7 CONCLUSIONS

NEURON is one of the most popular tools in the field of computational neuroscience for the simulation of morphologically detailed neural networks. We presented here an analysis of the diverse sources of error that can affect the results of NEURON simulations. Particular attention has been devoted to the numerical error arising from space and time discretization of the differential equations representing the mathematical model of the evolution of the membrane potential in a dendrite.

We examined the finite difference scheme and the numerical integration methods used in the current implementation of NEURON, and performed numerical experiments to investigate the orders of convergence of these schemes. In particular, for the time integration method we observed that the expected second order convergence was spoiled by the presence of singularities

in the solution and due to the simplifications introduced to eliminate the nonlinearities arising from the AMPA/NMDA synapse model.

We have presented here some techniques for handling the discontinuities in the system of ordinary differential equations and for addressing the nonlinearity in the AMPA/NMDA synapse model. These techniques allow the recovery of quadratic convergence without introducing extra computational cost. Moreover, we proposed the use of a second order Padé approximation for the computation of the ion channel gate states which reduces the computational cost without loss of precision.

Error estimators based on Zienkiewicz–Zhu patch recovery and Richardson extrapolation were presented, allowing a posteriori estimations of the errors introduced in space and time.

These methods have been validated numerically on a simple branched neuron model, demonstrating the gains in convergence order over the existing NEURON implementation. We plan to incorporate these methods into a future release of the NEURON simulator.

8 ACKNOWLEDGEMENTS

The work was supported by the EPFL Blue Brain Project Fund and the ETH Board funding to the Blue Brain Project.

REFERENCES

[1] Blackman, Arne V., et al. “A comparison of manual neuronal reconstruction from biocytin histology or 2-photon imaging: morphometry and computer modeling.” *Frontiers in neuroanatomy* 8 (2014).

[2] Bossetti, Chad A., Merrill J. Birdno, and Warren M. Grill. “Analysis of the quasi-static approximation for calculating potentials generated by neural stimulation.” *Journal of neural engineering* 5.1 (2007): 44.

[3] Carnevale, Nicholas T., and Michael L. Hines. *The NEURON book*. Cambridge University Press, 2006.

[4] Chung, Kwanghun et al. “Structural and molecular interrogation of intact biological systems.” *Nature* 497.7449 (2013): 332-337.

[5] Druckmann, Shaul, et al. “A novel multiple objective optimization framework for constraining conductance-based neuron models by experimental data.” Frontiers in neuroscience 1 (2007): 1.

[6] Goldman, Daniel, and Tasso J. Kaper. “N th-order operator splitting schemes and nonreversible systems.” *SIAM journal on numerical analysis* 33.1 (1996): 349-367.

[7] Hairer, Ernst, Syvert Paul Nørsett, and Gerhard Wanner. *Solving Ordinary Differential Equations I: Nonstiff problems*. Springer Verlag, 2008.

[8] Hairer, Ernst, Syvert Paul Nørsett, and Gerhard Wanner. *Solving Ordinary Differential Equations II: Stiff and differential-algebraic problems*. Springer Verlag, 2010.

[9] Hines, Michael. “Efficient computation of branched nerve equations.” *International journal of bio-medical computing* 15.1 (1984): 69-76.

[10] Hodgkin, Alan L., and Andrew F. Huxley. "A quantitative description of membrane current and its application to conduction and excitation in nerve." *The Journal of physiology* 117.4 (1952): 500.

[11] Krichmar, Jeffrey L., et al. "Effects of dendritic morphology on CA3 pyramidal cell electrophysiology: a simulation study." Brain research 941.1 (2002): 11-28.

[12] Lindsay, K. A., J. R. Rosenberg, and G. Tucker. "From Maxwell's equations to the cable equation and beyond." *Progress in biophysics and molecular biology* 85.1 (2004): 71-116. w to denote units of dimensionless

[13] Larsson, Jonas. "Electromagnetics from a quasistatic perspective." *American Journal of Physics* 75.3 (2007): 230–239.

[14] Markram, Henry, et al. "Reconstruction and simulation of neocortical microcircuitry." *Cell* 163.2 (2015): 456-492.

[15] Ovcharenko, Aleksandr, et al. "Simulating Morphologically Detailed Neuronal Networks at Extreme Scale.", ParCo15 Conference, Edinburgh, Scotland, 2015.

[16] Plonsey, Robert, and Dennis B. Heppner. "Considerations of quasi-stationarity in electrophysiological systems." *The Bulletin of mathematical biophysics* 29.4 (1967): 657-664.

[17] Quarteroni, Alfio, and Alberto Valli. *Numerical approximation of partial differential equations*. Vol. 23. Springer Science & Business Media, 2008.

[18] Wang, Yun, et al. "Anatomical, physiological, molecular and circuit properties of nest basket cells in the developing somatosensory cortex." *Cerebral Cortex* 12.4 (2002): 395-410.

[19] Sherman-Gold, Rivka. The Axon Guide for Electrophysiology & Biophysics: Laboratory Techniques. Axon Instruments, 1993.

[20] Van Geit, Werner, Erik De Schutter, and Pablo Achard. "Automated neuron model optimization techniques: a review." Biological cybernetics 99.4-5 (2008): 241-251.

[21] Zienkiewicz, O. C., and J. Z. Zhu. "The superconvergent patch recovery (SPR) and adaptive finite element refinement." *Computer Methods in Applied Mechanics and Engineering* 101.1 (1992): 207-224.